

February 1973

On a Tokamak with an  
Immaterial Separatrix Limiter

G. Lehner and F. Pohl

IPP III/6 February 1973

**MAX-PLANCK-INSTITUT FÜR PLASMAPHYSIK**  
**GARCHING BEI MÜNCHEN**



# MAX-PLANCK-INSTITUT FÜR PLASMAPHYSIK

## GARCHING BEI MÜNCHEN

On a Tokamak with an  
Immaterial Separatrix Limiter

G. Lehner and F. Pohl

IPP III/6 February 1973

*Die nachstehende Arbeit wurde im Rahmen des Vertrages zwischen dem  
Max-Planck-Institut für Plasmaphysik und der Europäischen Atomgemeinschaft über die  
Zusammenarbeit auf dem Gebiete der Plasmaphysik durchgeführt.*



IPP III/6

G. Lehner  
F. Pohl

On a Tokamak with an  
Immaterial Separatrix  
Limiter

(in English)

February 1973

### Abstract

Present-day Tokamak experiments suffer from serious disadvantages due to the presence of a material limiter, the shell providing the equilibrium, and the transformer with its flux problems. Perhaps the most feasible solution of the limiter problem could be obtained by using a magnetic separatrix as an immaterial limiter as proposed by FENEBERG. The examples discussed in the present report indicate that the multipole currents used to generate such a separatrix configuration can also solve the other problems, i.e. they can be chosen such that they provide plasma equilibrium and also serve as primaries of an air-core transformer. Another advantage of such a Tokamak machine is that it can be built with an axisymmetric divertor.



## 1) Introduction

The plasma parameters achieved in Tokamak experiments present an interesting step towards more efficient plasma confinement.

On the other hand, present-day Tokamak experiments suffer from some serious disadvantages due to the presence of a material limiter within the discharge vessel, the shell providing the equilibrium, and the transformer and its magnetic flux problems.

The effects produced by the limiter are not well known. The limiter may be responsible for some features of Tokamak discharges which are not yet understood. The plasma equilibrium in a Tokamak slowly changes with time and the plasma thus interacts with the limiter, which continually peels off layers of plasma. Under this circumstances interpretations of plasma particle or energy losses in terms of diffusion of any type, which are very popular these days, are not necessarily very conclusive. The limiter may also disturb the axisymmetry of the discharge. Thus, answers to the question how important axisymmetry is are not easily obtained from Tokamaks involving limiters. Another point of as yet unresolved discussion is whether the limiter has an influence on the stability or not. Furthermore, a final Tokamak reactor cannot be based on the usual limiter concept.

There are thus many reasons for developing Tokamaks without the present material limiter. Several proposals how to avoid a material limiter or at least its unwanted



consequences have been made: rapidly removable limiters, adiabatic compression of the plasma away from the wall, etc. Perhaps the most feasible solution of the problem could be obtained by using a magnetic separatrix as an immaterial limiter as proposed by FENEBERG /1/.

Such a separatrix can be obtained in many ways by superimposing the plasma magnetic fields and the magnetic fields from well chosen currents in azimuthal conductors outside the plasma. The separatrix has to divide the space within the discharge vessel into two different regions, one of closed magnetic surfaces completely within the vessel and another between the first one and the walls of the vessel in which the magnetic field lines are not contained but leave the vessel through the wall. The high-density high-temperature plasma would then mainly be contained within the inner region. Particles diffusing across the separatrix and entering the external region would rapidly be lost to the walls or to a connected divertor, so that in this external region one would have a plasma of low density (figure 1).

It is an attractive feature of such configurations that a new degree of freedom is added to the usual Tokamak design, which could result in some further advantages besides the elimination of the material limiter. If the currents in the outside conductors can be well controlled they can also provide the magnetic fields necessary for equilibrium, i.e. one could avoid the shell used for establishing the equilibrium in most Tokamaks up to now, except the Princeton ATC-Tokamak /2/ and the Russian TO-1 Tokamak /3/. Indeed the use of separatrix configurations would be more difficult with a shell than



without a shell because image currents induced in the shell tend to cancel the influence of the applied controlling currents whenever they change with time. One also has the freedom to shape the plasma cross section quite arbitrarily, i.e. to produce, for instance, elongated cross sections, which seem to have better stability properties than circular ones. In view of the reactor application it should be mentioned that this concept rather naturally leads to an extension into axisymmetric divertors.

For all these reasons we consider magnetic field configurations produced by azimuthal plasma currents together with superimposed external currents as schematically described by the example in figure 1.

To summarize, such a Tokamak would have the following properties:

- 1) no material limiter
- 2) no shell
- 3) no iron core but an air core transformer
- 4) the plasma aspect ratio  $r/R$  can be made favourably large
- 5) it can be used with an axisymmetric divertor
- 6) a large variety of cross sections is possible, though it has to be mentioned that the flexibility in producing different cross sections in one machine is rather limited.

The following discussion does not aim directly at real plasma equilibria. The plasma will be represented by given current density distributions. The reason for this is that the choice of different possible equilibria is overwhelmingly large and that it is not known which of



the many possible equilibria should be chosen as being particularly representative. On the other hand, a given current distribution in the plasma can usually be made consistent with some special equilibrium by only very minor changes which only very slightly alter the resulting field, the separatrix etc. For reasons of simplicity we start discussing some properties of corresponding linear configurations (in section 2) before going on to see what happens when we bend them into toroidal ones (in section 3).

## 2) Linear Configurations

We discuss the properties of a magnetic field produced by parallel line currents arranged as described in Figure 2. Along the z-axis of a Cartesian system of coordinates we have a line current  $J_0$ , which represents the plasma current in this extremely simplified model. It is surrounded by n conductors distributed uniformly, i.e. with equal angles  $2\pi/n$  between them, on a cylinder of radius  $r_0$ . Each of these n conductors carries the multipole current  $J_M$ . The resulting magnetic field can be described by only one component of the vector potential  $\vec{A}$ , i.e. by

$$A_z(x, y) = \frac{\mu_0}{2\pi} \left\{ J_0 \ln \sqrt{x^2 + y^2} + J_M \sum_{i=0}^{n-1} \ln \sqrt{(x-x_i)^2 + (y-y_i)^2} \right\} \quad (1)$$

For each i we have

$$x_i^2 + y_i^2 = r_0^2 \quad (2)$$



Introducing cylindrical coordinates  $r, \varphi, z$  and evaluating the sum in eq. (1) we obtain

$$A_z(r, \varphi) = \frac{U_0}{4\pi} \left\{ J_0 \ln r^2 + J_M \ln \left[ r^{2n} - 2r^n r_0^n \cos(n\varphi) + r_0^{2n} \right] \right\} \quad (3)$$

The magnetic fields are then

$$B_r = \frac{1}{r} \frac{\partial}{\partial \varphi} A_z \quad (4)$$

$$B_\varphi = - \frac{\partial}{\partial r} A_z \quad (5)$$

The stagnation points of the field are given by

$$B_r = B_\varphi = 0 \quad (6)$$

It is found that for stagnation points

$$\cos(n\varphi) = \pm 1 \quad (7)$$

i.e. stagnation points are situated either on lines connecting the center current with one of the multipole currents ( $\cos(n\varphi)=1$ ) or on lines between at half-angles ( $\cos(n\varphi)=-1$ ). The situation of the stagnation points on these lines depends on the relative size of the currents  $J_0$  and  $J_M$ . We describe it by a parameter  $\alpha$  :

$$\alpha = - \frac{J_0}{n J_M} \quad (8)$$



$\alpha$  is positive for antiparallel currents and negative for parallel ones. For  $\alpha = 1$  the total current is just zero. Calculating the radii of the stagnation points  $r_s$ , we get

$$I) \left(\frac{r_s}{r_0}\right)^n = \frac{\alpha}{\alpha - 1} \quad \alpha = \frac{1}{1 - \left(\frac{r_0}{r_s}\right)^n} \quad \text{if } \alpha > 1 \text{ or } \alpha \leq 0 \quad (9)$$

$$\cos(n\varphi) = 1$$

$$II) \left(\frac{r_s}{r_0}\right)^n = \frac{\alpha}{1 - \alpha} \quad \alpha = \frac{1}{1 + \left(\frac{r_0}{r_s}\right)^n} \quad \text{if } 0 \leq \alpha \leq 1 \quad (10)$$

$$\cos(n\varphi) = -1$$

Figure 3 indicates the location of the stagnation points as a function of the parameter  $\alpha$ . Figure 4 gives examples of the different magnetic configurations which are possible. Only two of the configurations [b) and e)] meet our requirement that the inner region be completely within the vessel, at least if we do not use strangely shaped cross sections for the discharge vessel.

Case b) is obtained for  $0 < \alpha < \frac{1}{2}$   $\frac{r_s}{r_0} = \sqrt[n]{\frac{\alpha}{1 - \alpha}}$  (11)

and case e) for  $0 > \alpha > -\infty$   $\frac{r_s}{r_0} = \sqrt[n]{\frac{\alpha}{\alpha - 1}}$  (12)

Even if toroidal effects are not included in the present discussion, these results already afford some useful information. Let us assume that we want to confine a plasma column in a linear configuration of this type. Let us also



assume as an example that  $r_s = \frac{2}{3} r_o$  is chosen in order to have enough space for the vessel and some distance between the inner region and the vessel. We can then calculate the following values for  $\alpha$ ,  $J_M$ ,  $nJ_M$ :

	$\alpha$	$J_M/J_o$	$nJ_M/J_o$	$\alpha$	$J_M/J_o$	$nJ_M/J_o$
n=4	0.165	-1.51	- 6.06	-0.246	1.01	4.06
n=8	0.0375	-3.34	-26.7	-0.0406	3.08	24.6
	Configuration of type 4 b)			Configuration of type 4 e)		

If the multipole currents become smaller than indicated in this table, the diameter of the separatrix bounding the inner region increases and the separatrix can no longer play its role as an immaterial limiter. The fact that the plasma current is represented by a line current at the moment does not essentially change the situation. We see that rather large currents are necessary and can draw the following conclusions:

- a) With parallel multipole currents (configuration 4 e) sufficiently small radii of the separatrix are somewhat easier to obtain than with antiparallel ones (conf. 4 b). On the other hand, stability considerations seem to indicate that antiparallel currents should be preferred. A simple analysis of rigid and parallel displacement of the plasma and its current such that the magnetic fluxes between any pair of conductors is kept constant gives stabilising contributions from antiparallel multipole currents and destabilising contributions from parallel ones. In any case antiparallel currents tend to push the plasma away, while parallel currents attract it.



- b) In both cases each multipole current  $J_M$  is of the order of the plasma current  $J_0$ , i.e. unfavourably large.
- c) The number of multipole currents  $n$  should be kept as small as possible. For instance,  $n=8$  requires much stronger currents than  $n=4$ .
- d) The actual requirements depend quite strongly on the ratio  $r_s/r_0$  which is necessary. If  $r_s$  approaches  $r_0$ , the requirements are relaxed, i.e. smaller currents are needed. So the distance between the plasma and the multipole conductors should be made as small as possible, i.e.  $r_s/r_0$  should be made as large as possible. This design condition can be more readily satisfied for a rather "fat" plasma and vessel system. The lower limit which can be approached in the antiparallel case is

$$\frac{r_s}{r_0} \rightarrow 1 \quad \text{with } \alpha \rightarrow \frac{1}{2} \quad nJ_M \rightarrow -2J_0$$

In order to keep the separatrix stationary during the operation cycle,  $\alpha$  has to be kept constant, i.e. the multipole currents should always be (at least approximately) proportional to the plasma current  $J_0$ , i.e. they should have the same time dependence. In the toroidal case to be discussed in the next section this has the consequence that the multipole rings have to be considered together with the transformer and actually form the primaries or part of the primaries of an air core transformer.



e) The use of a copper shell would increase the difficulties. Because there is not much space available shell and multipole conductors would be rather close to one another and larger currents than without shell would be necessary because image currents in the shell tend to cancel the effect of the multipole currents by which they are produced. Thus, it seems natural to avoid the shell completely and to arrange the multipole conductors in such a manner that they also provide the fields for plasma equilibrium.

To conclude this section, let us discuss the influence of the image currents just mentioned.

For sufficiently short times (depending on the thickness of the shell) the shell can be assumed to be infinitely conducting. The field inside the shell then can be represented by image currents:

$$J_M^I = - J_M \quad (13)$$

at the mirror points of the multipole conductors, i.e. at the same angles  $\varphi$  and at the radius

$$r_1 = \frac{r_{cu}^2}{r_0} \quad (14)$$

where  $r_{cu}$  is the radius of the (copper) shell.

The vector potential including these image currents is

$$A_z(r, \varphi) = \frac{\mu_0 J_0}{4\pi} \ln r^2 + \frac{\mu_0 J_M}{4\pi} \ln \frac{r^{2n} - 2r^n r_0^n \cos(n\varphi) + r_0^{2n}}{r^{2n} - 2r^n r_1^n \cos(n\varphi) + r_1^{2n}} \quad (15)$$

Discussing the problem as in the preceding case, we look for the stagnation points. The different possible cases



may be classified by using the parameter

$$f = \frac{r_1^{\frac{n}{2}} - r_0^{\frac{n}{2}}}{r_1^{\frac{n}{2}} + r_0^{\frac{n}{2}}} < 1 \quad (16)$$

The situation of the stagnation points is described in fig. 5 and examples of the different field configurations are shown in fig. 6. Only the cases b) and g) in fig. 6 are of interest here. We can calculate

for case b) 
$$\alpha = \frac{r_s^n (r_1^n - r_0^n)}{r_s^{2n} + r_s^n (r_1^n + r_0^n) + r_0^n r_1^n} \quad (17)$$

and for case g) 
$$\alpha = \frac{-r_s^n (r_1^n - r_0^n)}{r_s^{2n} - r_s^n (r_1^n + r_0^n) + r_0^n r_1^n} \quad (18)$$

In the limit  $r_1 \rightarrow \infty$  eq. (17) yields eq. (10), and (18) yields (9). Equations (17) and (18) describe how  $\alpha$  decreases ( $J_M$  increases) as  $r_0$  approaches  $r_1$  i.e. as the multipole currents come closer to the shell. In, for instance, the antiparallel case b) we get for

$$n = 4, \quad \frac{r_s}{r_0} = \frac{2}{3}$$

the following values for  $\alpha$  and  $J_M$  for different values of  $\frac{r_1}{r_0}$

$r_1/r_0$	$\alpha$	$J_M/J_0$	$nJ_M/J_0$
$\infty$	0.165	-1.51	-6.06
2	0.153	-1.63	-6.54
1.1	0.046	-5.43	-21.7
1	0	$\infty$	$\infty$



These values confirm that a shell may lead to very strong multipole currents if it is close to the multipole conductors and should therefore be avoided.

### 3) Axisymmetric Toroidal Configurations

In the toroidal case analytic results as in the linear case cannot be obtained, but the linear results remain approximately true and may thus serve as a first orientation with respect to the order of magnitude of currents necessary to obtain the desired configurations. Details of the field configurations are obtained by plotting the lines using the fact that the quantity  $r A_\varphi$  is a flux function, i.e.:

$$\Psi = r A_\varphi(r, z) = \text{const. along field lines} \quad (19)$$

Poloidal field components  $B_r, B_z$  are considered only in planes  $\varphi = \text{const.}$  Superimposed azimuthal fields (i.e. the main Tokamak field) do not change the magnetic surfaces.  $B_r$  and  $B_z$  are obtained from  $A_\varphi$  by

$$B_r = - \frac{\partial}{\partial z} A_\varphi \quad (20)$$

$$B_z = \frac{1}{r} \frac{\partial}{\partial r} (r A_\varphi) \quad (21)$$

$A_\varphi(r, z)$  is computed by summing or integrating all the contributions from the azimuthal currents involved. The necessary integrations were performed by several methods. Furthermore, some results obtained with our programmes were compared with results obtained with a programme written



by R. POEHLCHEN /4/. For a single azimuthal line current  $J$  at  $r_0, z_0$  (Fig. 7) we have

$$A_{\varphi}(r, z) = \frac{\mu_0 J}{\pi k} \sqrt{\frac{r_0}{r}} \left[ \left(1 - \frac{k^2}{2}\right) K - E \right] \quad (22)$$

$K$  and  $E$  are complete elliptic integrals,

$$K(k) = \int_0^{\pi/2} d\vartheta \frac{1}{\sqrt{1 - k^2 \sin^2 \vartheta}} \quad (23)$$

$$E(k) = \int_0^{\pi/2} d\vartheta \sqrt{1 - k^2 \sin^2 \vartheta} \quad (24)$$

while  $k$  is given by

$$k = \sqrt{\frac{4rr_0}{(r+r_0)^2 + (z-z_0)^2}} \quad (25)$$

Fig. 8 shows two computed examples of toroidal field configurations which correspond to the linear case shown in Fig. 4 b). These results may appear surprising at first sight, but they are natural consequences of going from the highly symmetric and therefore degenerate linear case to the less symmetric toroidal one. The loss of symmetry leads to a splitting of the separatrices into more separatrices and to the appearance of topologically new regions between them. The region of main interest to us, i.e. the center region containing the plasma also changes some of its properties. While it contains four stagnation points in the linear case, it contains here for example one (8 b) or two (8 a) stagnation points. Fig. 8 is obtained for equal multipole currents  $J_M$ .



In the toroidal case there is actually no reason to have equal currents in the multipole conductors. In general, the multipole currents will be different in the following except for symmetry with respect to the equatorial plane, which will be sustained. One thus obtains a large variety of different configurations which cannot be discussed exhaustively. We can only discuss examples which are more or less arbitrarily chosen.

The plasma has a relatively large diameter and cannot really be represented by a line current. Unfortunately, the plasma current profile cannot be predicted. We thus restrict ourselves to a relatively simple model. We assume that the inner plasma region - i.e. inside the inner separatrix - carries a current of constant density  $j_1$ . The space between this separatrix and the discharge vessel is supposed to be filled with a lower density plasma and a current of lower but also constant density  $j_2$  ( $j_2 \leq j_1$ ). This model is schematically represented in Fig. 9. Configurations corresponding to this model can be computed by iteration. Starting with a relatively arbitrary configuration (where the multipole currents are, however, chosen such that the separatrix has a reasonable diameter and a position approximately at the center of the vessel), one computes the magnetic fields and the separatrix produced by these currents. In the next step the same total plasma current is distributed with a jump of  $j$  at the old separatrix and a new separatrix is computed etc. The procedure finishes, when the separatrix no longer changes. If the initial configuration is well chosen, only few steps are necessary in some cases, while there are also cases for which the iteration does not seem to converge. If it does converge, we get what is called in the following a "compatible" configuration. The word "compatible"



as used here therefore should not be misunderstood. It has, for instance, no relation to the MHD equilibrium problem.

The series of figures 10 to 16 shows some of the steps on the way from simple configurations with line currents only to compatible configurations in the sense just defined. Figure 10, to begin with, is a more detailed plot of a configuration similar to that in fig. 8b. For later use we also plot the magnetic field  $B_z(r)_{z=0}$ , i.e. the vertical field on the equatorial plane as a function of  $r$ . Quite unrealistically, the plasma is represented by a line current. We now replace the line current by an extended current of circular cross section with variable diameter and constant current density. As long as the diameter is smaller than the diameter of the separatrix this has no strong influence on the configuration. For sufficiently large diameters of the current carrying plasma loop, however, the inner region rapidly contracts (fig. 11) and finally disappears (fig. 12). Figures 10, 11, 12 are for equal multipole currents. A configuration as in fig. 12 is not what we want to discuss. The effect of the increasing diameter of the current carrying plasma region on the separatrix can, however, be more or less compensated by superimposing a homogeneous field  $B_z$  of the right magnitude and sign. From the plot of  $B_z(r, z)_{z=0}$  one can deduce the field which is necessary to shift the magnetic axis back into the center of the vessel. Fig. 13 shows that superimposing the right field  $B_z$  leads to the reappearance of the separatrix which disappeared in fig. 12. The same effect can be achieved by using different currents in the multipole rings (see fig. 14). Another compatible configuration with  $j_1/j_2 = 7.4$  is shown in fig. 15. Fig. 16 finally shows a somewhat different configuration in which additional currents (a parallel current on the inside and



an antiparallel one on the outside) are used for improved shaping of the separatrix and a slight reduction of the other multipole currents.

It is not clear if the model chosen is a very representative one. As already mentioned, the current density profile in Tokamak discharges is not very well known and it is not possible either to influence a discharge in such a manner that a prescribed profile is produced. But it seems that the model is reasonable in the sense that the configuration does not drastically change if the current distribution is somewhat changed.

Fig. 17 shows separatrices of three different compatible cases with the same total plasma current but different values of the current densities  $j_1$  and  $j_2$ .

We have not yet taken into account the plasma equilibrium problem. Qualitatively, it can be stated that the perpendicular field applied in fig. 13 (homogeneous superimposed field) and also in fig. 14, 15, 16 (here produced by the multipole currents and their differences) is in the right direction, i.e. it produces a force on the plasma counteracting the hoop force. Furthermore, we can ask if the configurations given may be in MHD equilibrium or not. For the sake of simplicity, we have assumed constant current densities in the two regions. This, however, implies that the configuration is certainly not in equilibrium precisely, because for any axisymmetric equilibrium the azimuthal plasma current is of the following form:

$$j_{\varphi} = r \frac{dp(\psi)}{d\psi} + \frac{1}{r} \frac{J(\psi)}{4\pi} \frac{dJ(\psi)}{d\psi} \quad (26)$$

where  $\psi$  is the flux function already defined (eq.19);  $p$  is the plasma pressure, a function of  $\psi$  only;  $J$ , also a function of  $\psi$  only, is closely related to the azimuthal magnetic field necessary:

$$J(\psi) = r B_{\varphi}(r, z) \quad (27)$$



According to eq.(26)  $j_\varphi$  cannot be constant on a magnetic surface in contradiction to our model assumption. But it can be shown that the arbitrary functions  $p(\psi)$  and  $J(\psi)$  can be chosen such that  $j_\varphi$  is almost constant on the magnetic surfaces. This means that only slight changes in the model current distributions are necessary to get current distributions which are consistent with special equilibria belonging to special functions  $p(\psi)$ ,  $J(\psi)$ . These slight changes of the current distributions would, in turn, also very slightly change the configurations plotted.

We therefore believe that our model does not lead to unrealistic examples as far as equilibrium considerations are concerned. In an actual experiment matters are more complicated. The real equilibrium cannot be predicted and it is also subject to change with time. Therefore, an experiment would need feedback control of the multipole currents such that at any time the right fields necessary for equilibrium are maintained. Now take, for instance, the configuration in fig.16 and let us choose  $p(\psi)$  and  $J(\psi)$  such that  $j_\varphi$  as given by eq.(26) is almost constant along the flux surfaces and plot, for instance,  $p$  as a function of  $r$  along the equatorial plane. The result is shown in fig. 18. In this example the maximum pressure at the magnetic axis is  $p = 3.2 \times 10^{+4} \text{ dyn/cm}^2$ . The corresponding poloidal  $\beta$  value is  $\beta \approx 1$ . This appears to be reasonable in comparison with experimental Tokamak results. As already mentioned, the multipole rings can be considered to be the primaries or part of the primaries of an air core transformer for the ohmic heating current. If we neglect the resistive losses - which is possible for sufficiently short times - the plasma current induced by the multipole currents is given by

$$J_p = - \frac{\sum_{k=1}^n L_{pk} J_k}{L_{pp}} \quad (28)$$

$L_{pk}$  is the mutual inductance between the multipole ring  $k$  with the current  $J_k$  and the plasma;  $L_{pp}$  is the self-inductance



of the plasma and  $J_p$  is the induced plasma current. To evaluate  $J_p$  from eq.(28), the problem has been simplified quite severely in order to avoid large computations.  $L_{pk}$  has been calculated as if the plasma were a line current in the center and  $L_{pp}$  has been calculated as if the plasma current density were constant within the vessel. In most cases treated the current  $J_p$  obtained is larger than the plasma current  $J_0$  chosen so as to obtain the desired configuration, i.e. the current  $J_p$  (when substituted for  $J_0$ ) would lead to a separatrix with too large a diameter not contained within the vessel. In these cases one would have to use correcting transformers which reduce the plasma current but do not disturb the magnetic configuration in the neighbourhood of the separatrix. There are, however, also cases where  $J_p$  is close to the current  $J_0$  assumed to get compatible configurations. In, for example, fig. 19a) we have  $J_0 = -100$  kA and  $J_p = -110$  kA, while in fig. 15a) we have  $J_0 = -100$  kA and  $J_p = -206$  kA. Thus, in fig. 19 the two currents  $J_0$  and  $J_p$  are approximately consistent, a fact which is due to the negative current at A.

By changing one or some of the currents in configurations as described above one can drastically change the topology of the configuration. Consider, for instance, fig. 19, which gives a comparison between three different cases with multipole arrangements as in fig. 16. All the currents are kept constant except the negative one between the plasma and the axis. As long as this current remains sufficiently weak, we get what has been discussed before and already shown in fig. 16. For a larger current (at A) the configuration switches over into an essentially different one. With a still larger current we get another configuration again. If we want to connect the separatrix with an axisymmetric divertor, this is an extremely important problem. In this case we have to make sure that the configuration does not switch over during the discharge from, for instance, the one of fig. 19a) to the one in fig. 19b). As far as the divertor is concerned, the



configuration of type 19a) is preferable because in this case one has space available for the divertor above and below the plasma, while in case 19b) the divertor would have to be placed between the plasma and the axis, where little space is available. This example shows that, when working with axisymmetric divertors of the type discussed here, one has to choose the parameters so that the currents are sufficiently far from currents at which such switching could occur. The principles discussed here can also be used to produce a large variety of plasma cross sections. Fig. 20 shows one example with a rather elongated cross section. It should be mentioned that in order to get cross sections of this type one needs quite a lot of currents to obtain reasonable shapes.

#### 4) Conclusions

The examples discussed above seem to show that it is possible with additional multipole currents to produce Tokamak configurations meeting several requirements at once:

- 1) A separatrix replaces the material limiter.
- 2) Fields for equilibrium are provided without use of a shell.
- 3) Multipole currents serve as primaries of an air core transformer.
- 4) The configuration can be connected with an axisymmetric divertor.

We feel that these facts could lead to an essentially improved Tokamak design not impeded by the parts which cause a great deal of trouble in present-day conventional Tokamaks (limiter, shell, iron core).

Obviously, the configurations chosen only serve as a few examples of a very large variety of possibilities. The final choice of a configuration would have to be based on additional considerations and experiments - concerning stability, for



instance, which we have not discussed here. Actually, some of the questions involved cannot be answered by purely theoretical considerations. Experiments will be very important. The authors feel that these questions should be treated in medium-sized Tokamaks before a really large Tokamak is built.

#### References

- |                       |  |
|-----------------------|--|
| /1/ W. Feneberg       | Phys. Lett. <u>36A</u> (1971) 125  |
| /2/ K. Bol et.al.     | Phys.Rev.Lett. <u>29</u> (1972) 1495   |
| /3/ Artemenkov et.al. | Proceedings of the Madison<br>Conf. 1971, Vol. <u>1</u> , 359<br>(Paper CN-28/C-3) |
| /4/ R. Poehlchen      | Report IPP 4/86 (1971)   |



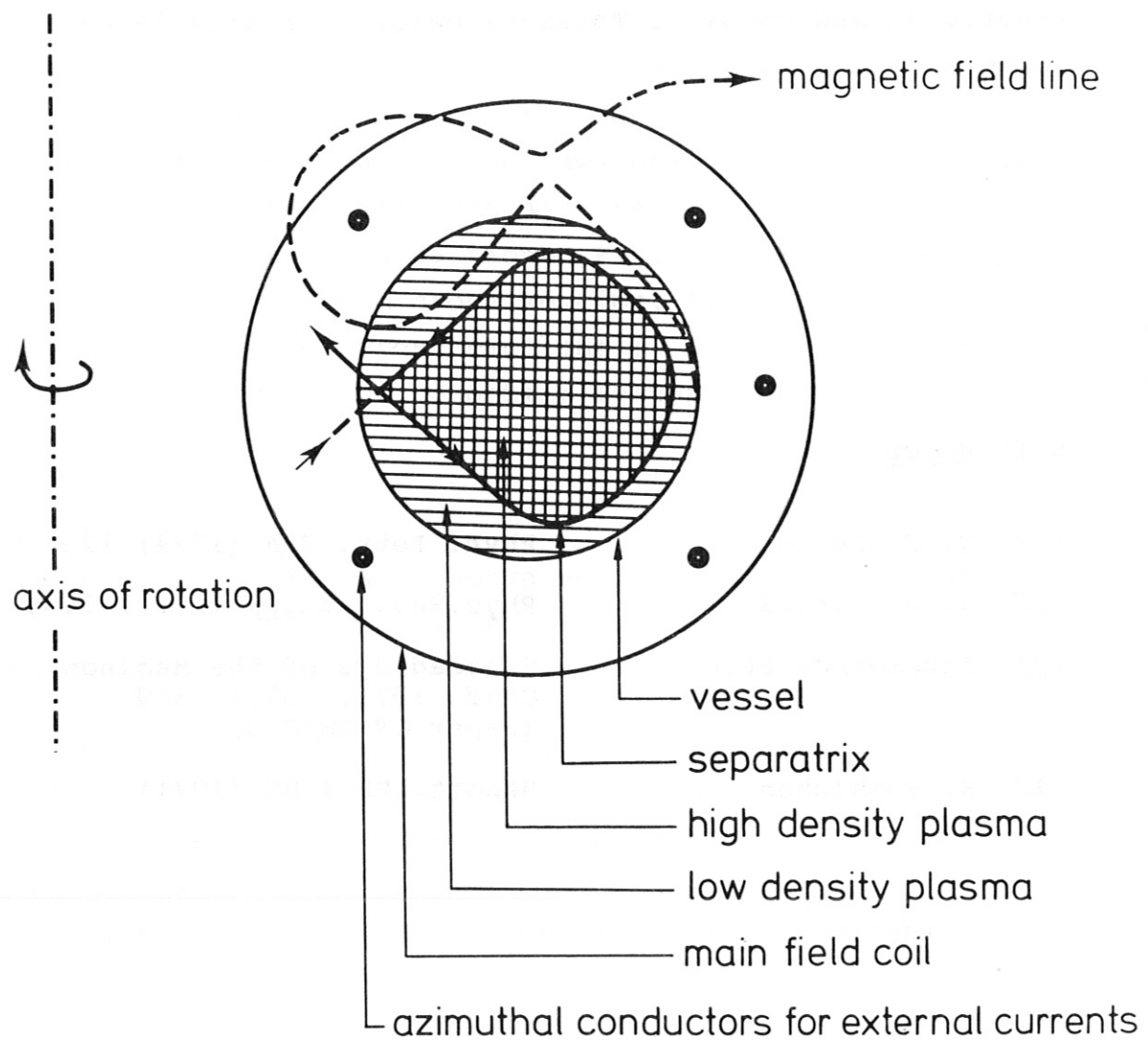


Fig.1 An example of a multipole Tokamak



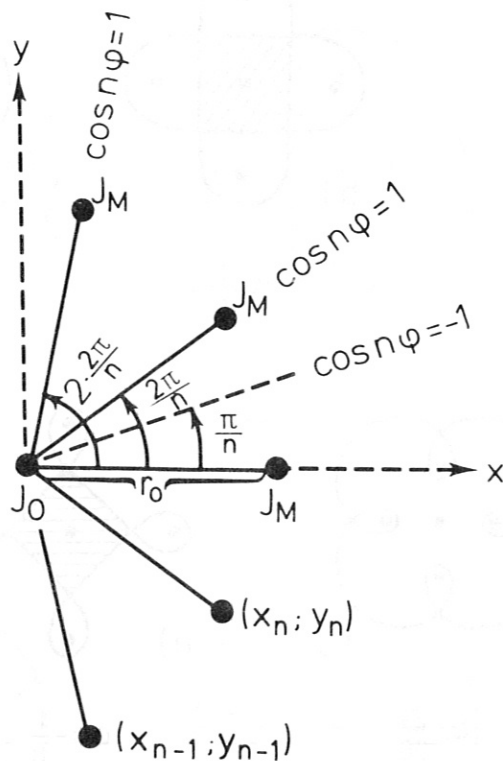


Fig.2 Center current surrounded by  
n "multipole" currents  $J_M$

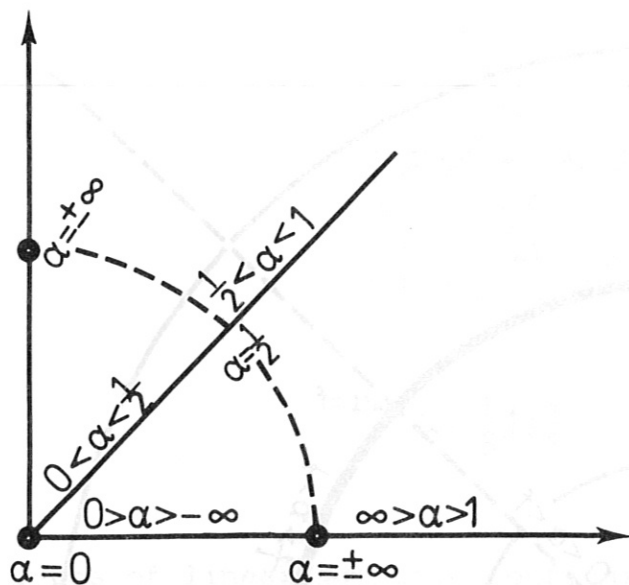


Fig.3 Location of the stagnation points for different values  
of  $\alpha$ .

The results given here for  $n=4$  are valid for any  $n$ .



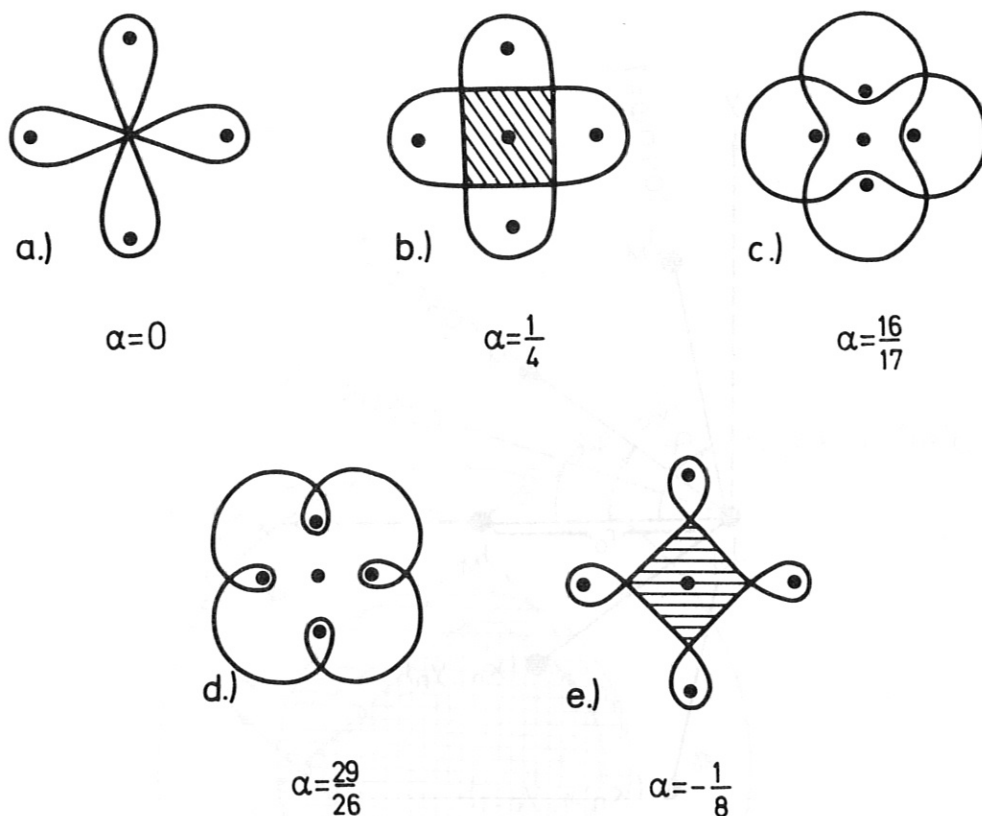


Fig.4 Types of linear magnetic configurations for  $n=4$ .  
 Type a) is obtained for  $\alpha=0$ , b) for  $0 < \alpha < \frac{1}{2}$ ,  
 c) for  $\frac{1}{2} < \alpha < 1$ , d) for  $\alpha > 1$ ,  
 and e) for  $\alpha < 0$

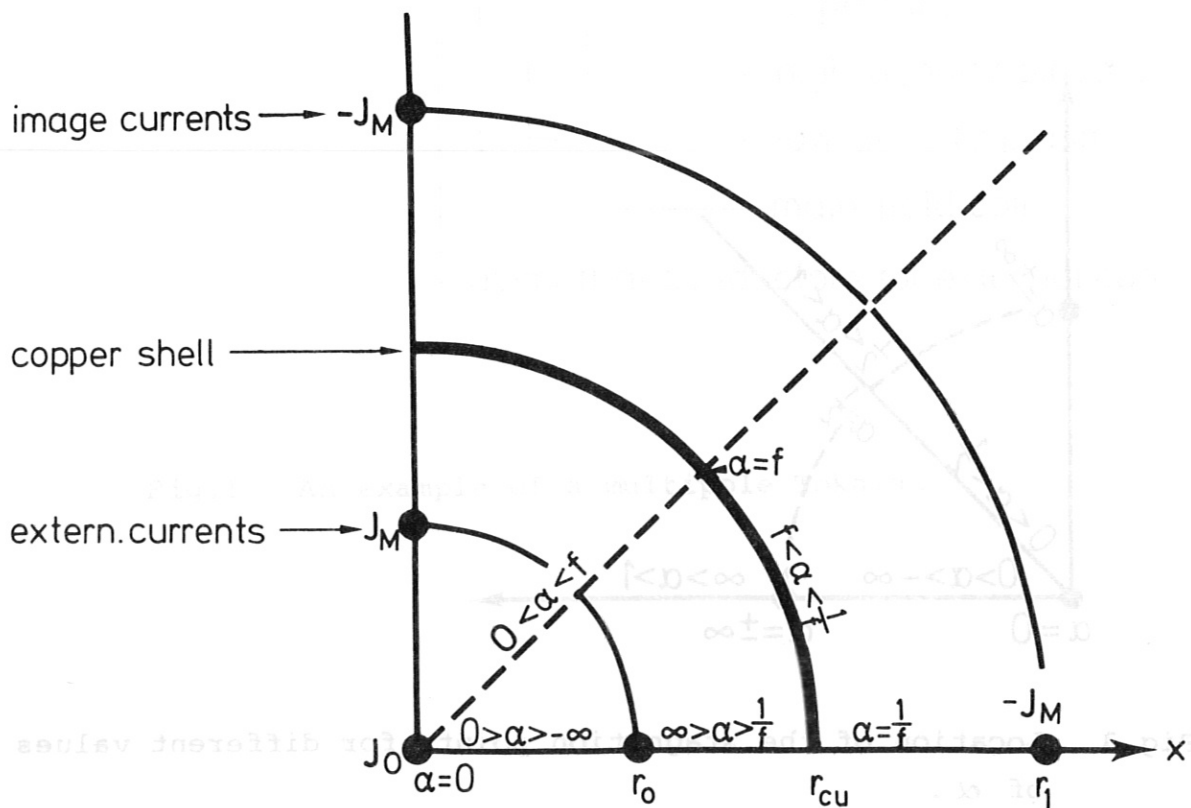
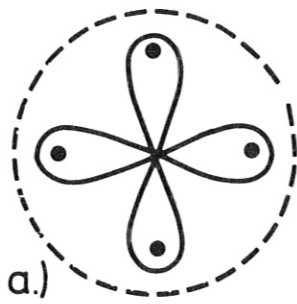
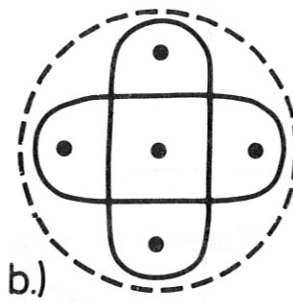


Fig.5 Location of stagnation points with shell

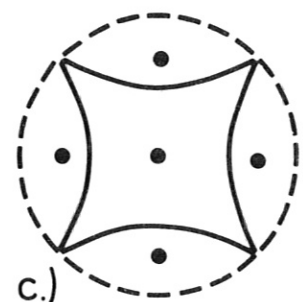




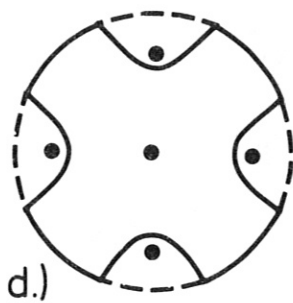
$$\alpha=0, f=\frac{3}{5}$$



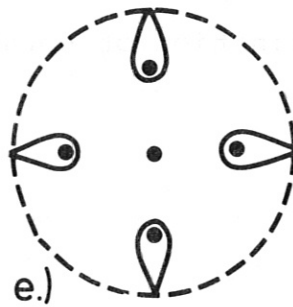
$$\alpha=\frac{1}{4}, f=\frac{3}{5}$$



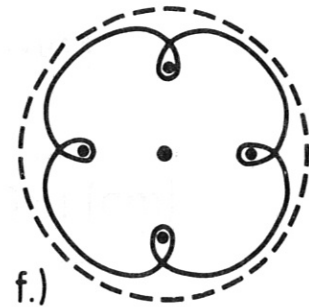
$$\alpha=f=\frac{3}{5}$$



$$\alpha=1, f=\frac{3}{5}$$



$$\alpha=\frac{5}{4}, f=\frac{4}{5}$$



$$\alpha=\frac{3}{2}, f=\frac{4}{5}$$



$$\alpha=-\frac{1}{8}, f=\frac{3}{5}$$

Fig.6 Types of linear magnetic configurations with shell.  
 Type a) is obtained for  $\alpha=0$ , b) for  $0 < \alpha < f$   
 c) for  $\alpha=f$ , d) for  $f < \alpha < \frac{1}{f}$   
 e) for  $\alpha = \frac{1}{f}$ , f) for  $\frac{1}{f} < \alpha < \infty$   
 and g) for  $\alpha < 0$



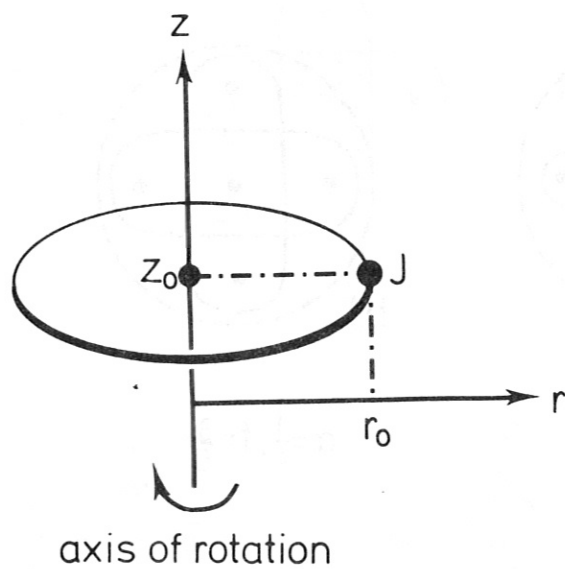


Fig.7 Definition of notation

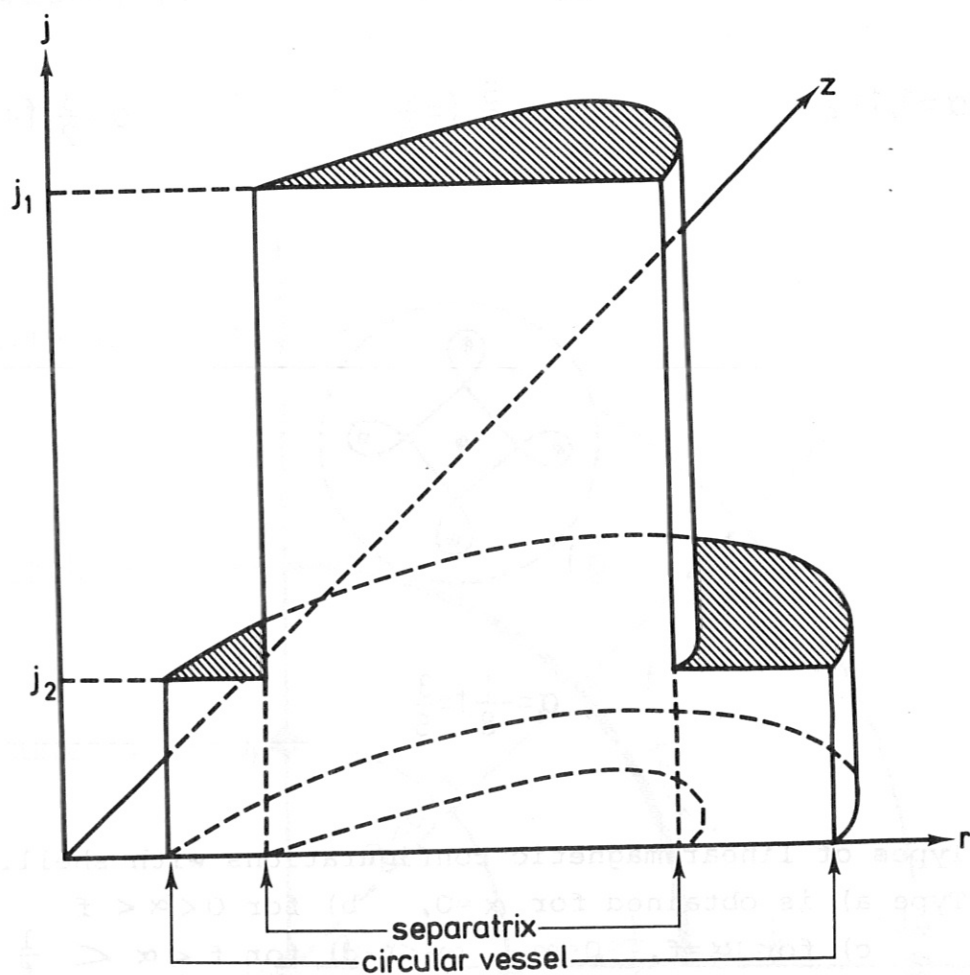


Fig.9 Model of current profile



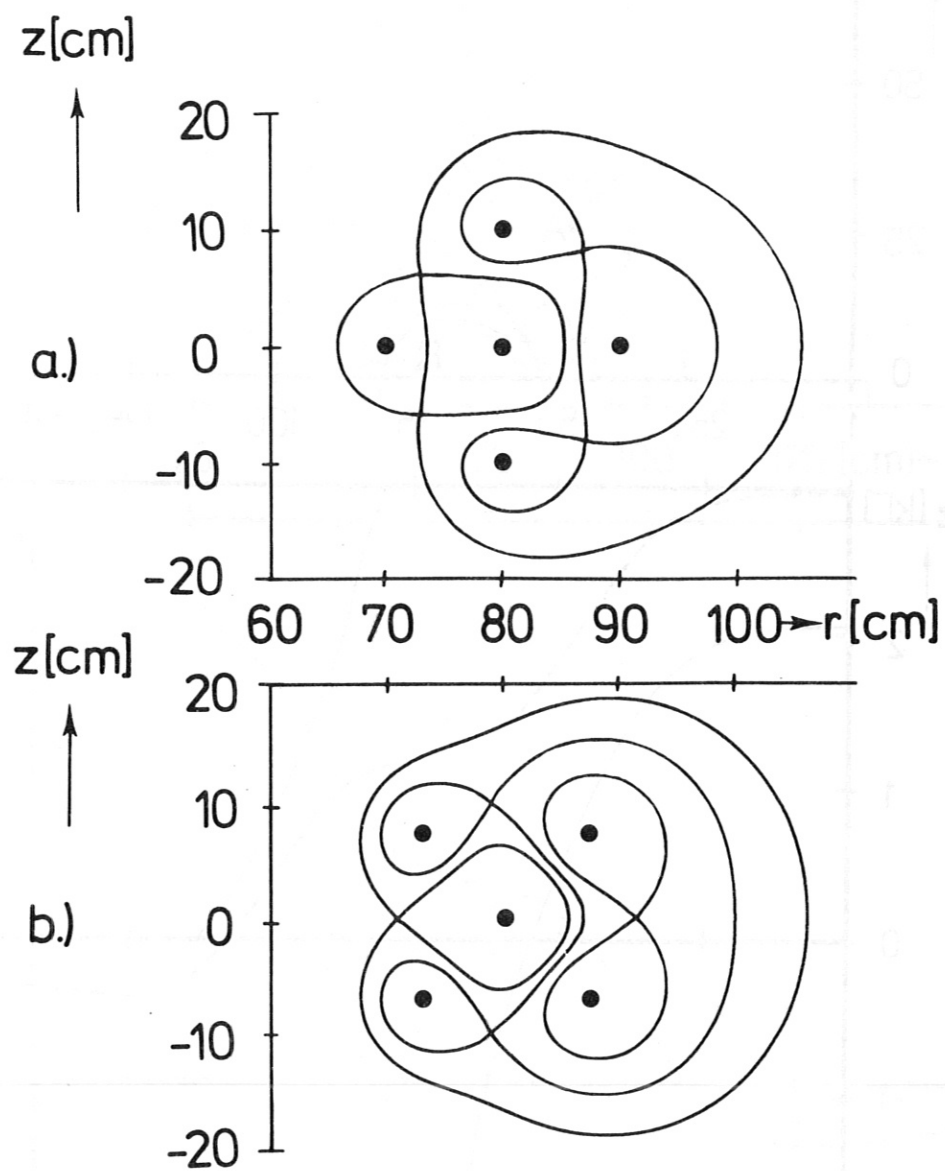


Fig.8 Two examples of toroidal field configurations for equal multipole currents  $J_M = -\frac{1}{2}J_0$  ( $\alpha = \frac{1}{2}$ )



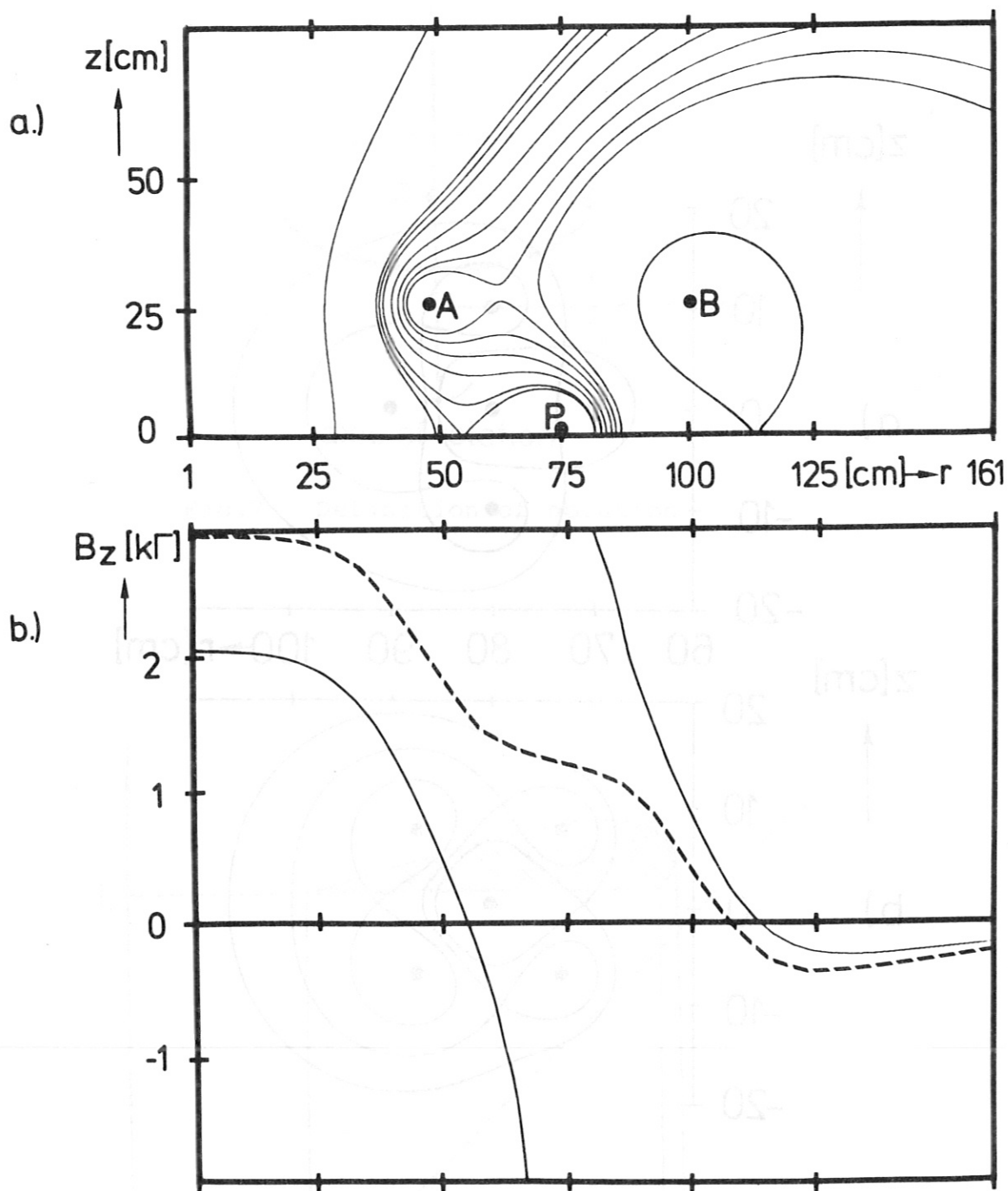


Fig.10 a) magnetic field lines in the r-z-plane  
 b)  $B_z(r, z=0)$  without plasma current (dashed line)  
 and including " " (solid " )  
 for  $n=4$  and the following currents

Conductor	Current (kA)	Location	
		r (cm)	z (cm)
P	-100	75.	0.
A	100	48.84	$\pm 26.16$
B	100	101.16	$\pm 26.16$



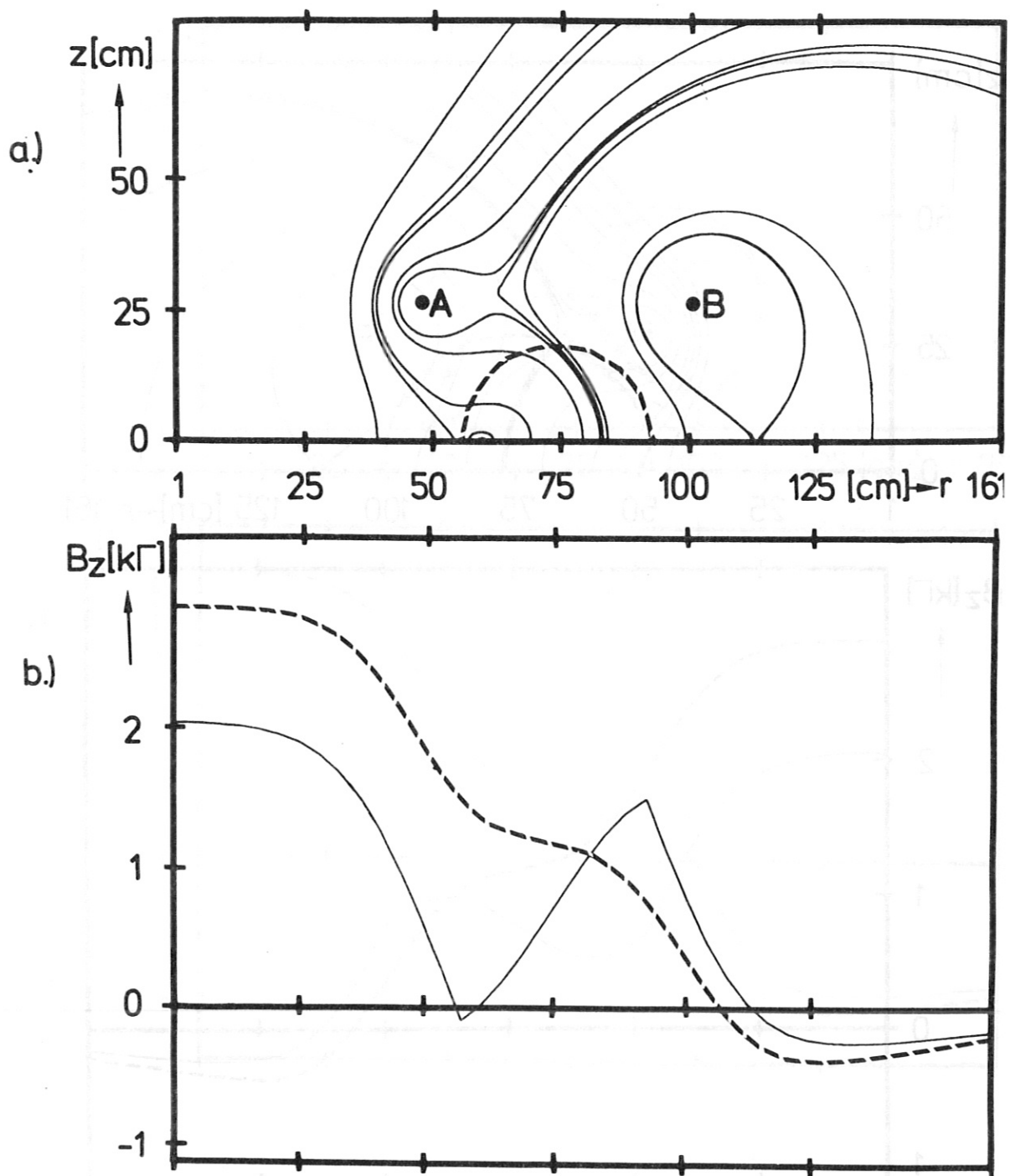


Fig.11 As fig.10, but the plasma is represented by a current of constant density within a region of circular cross section (plasma radius = 18 cm)



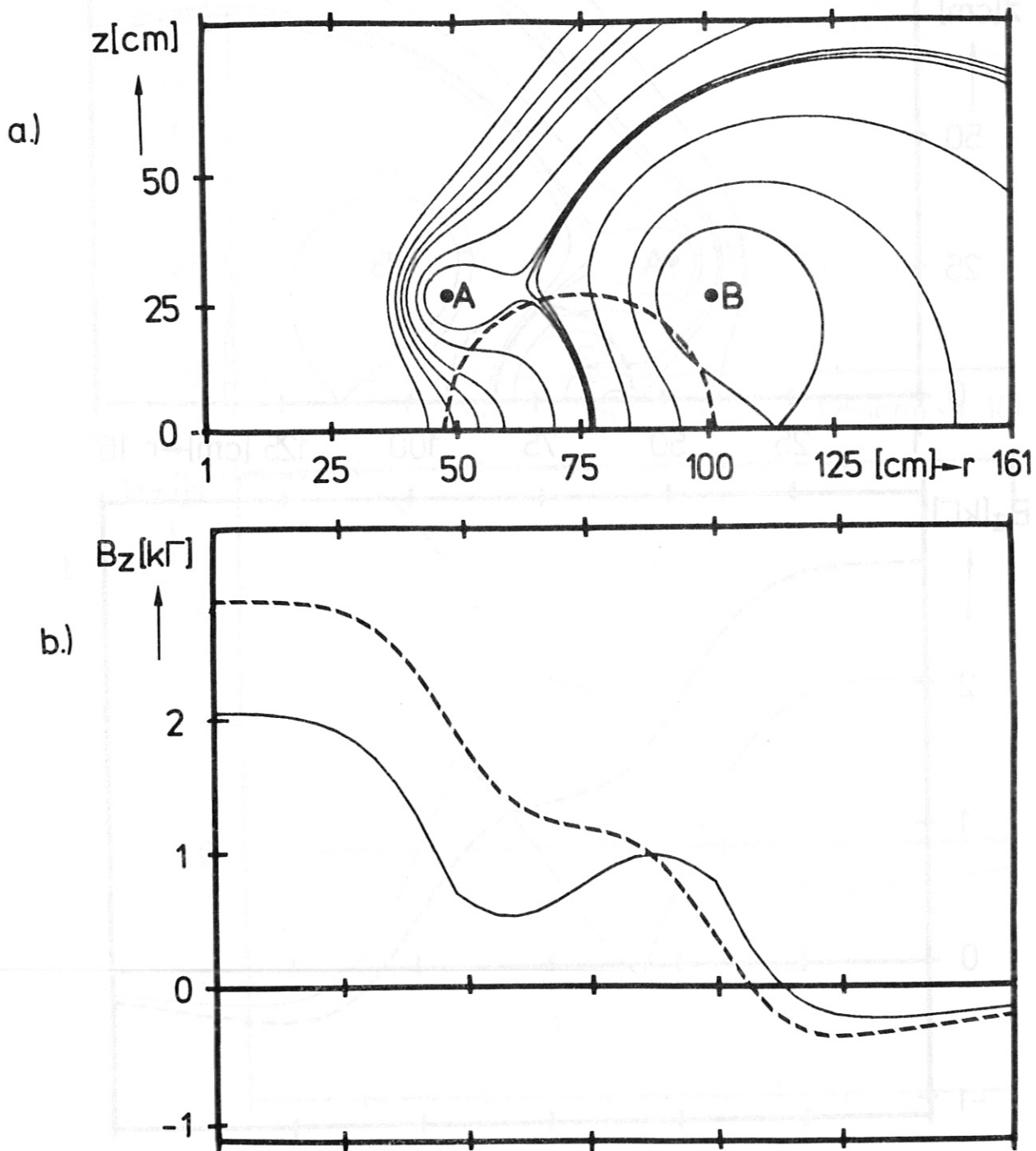


Fig.12 As fig.11, but with plasma radius 26.5 cm



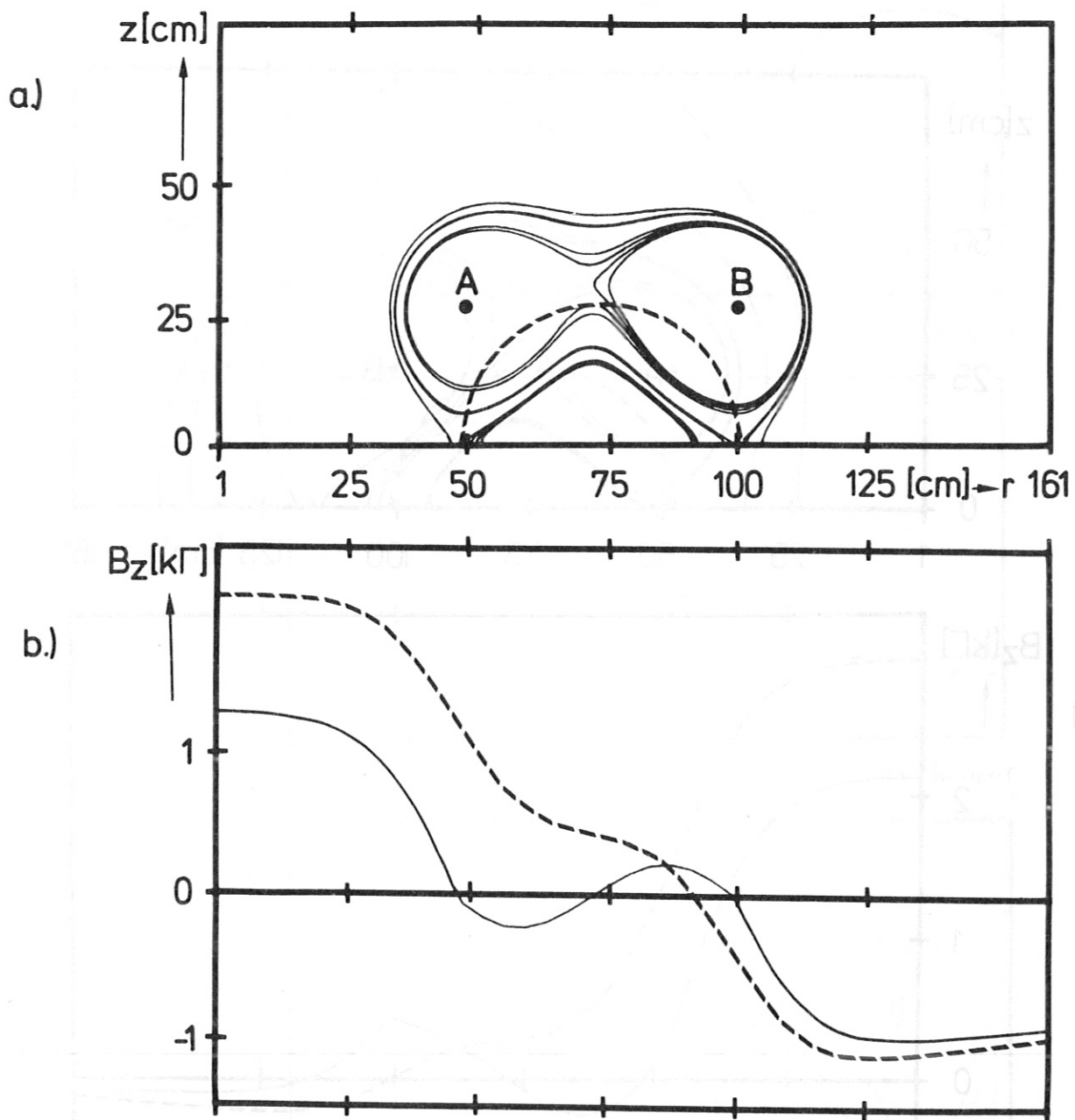


Fig.13 As fig.12, but with superimposed homogeneous field of - 770 gauss



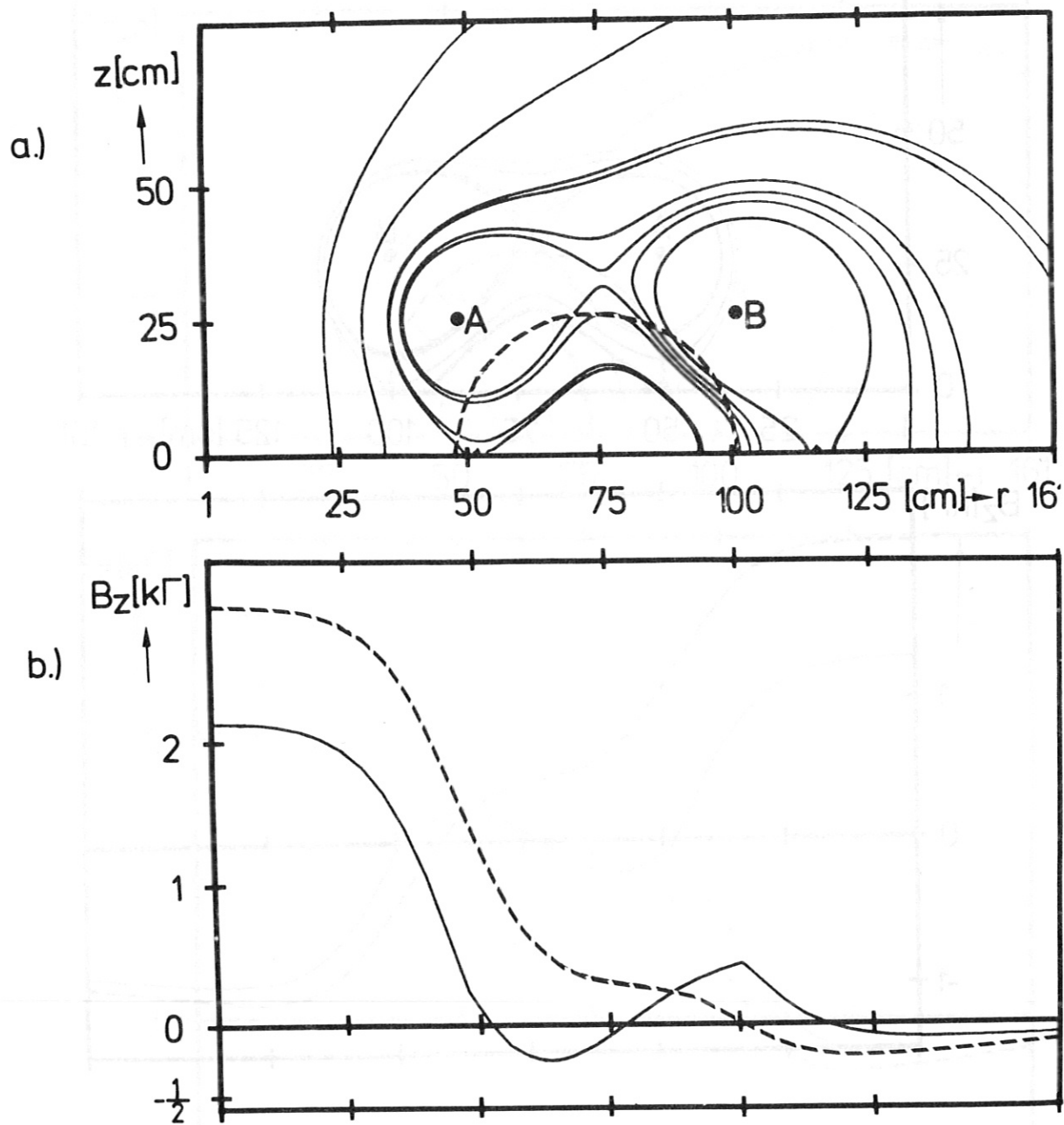


Fig.14 As fig.12, but with the following multipole currents

Conductor	Current (kA)	Location	
		r (cm)	z (cm)
A	144	48.84	$\pm 26.16$
B	40	101.16	$\pm 26.16$



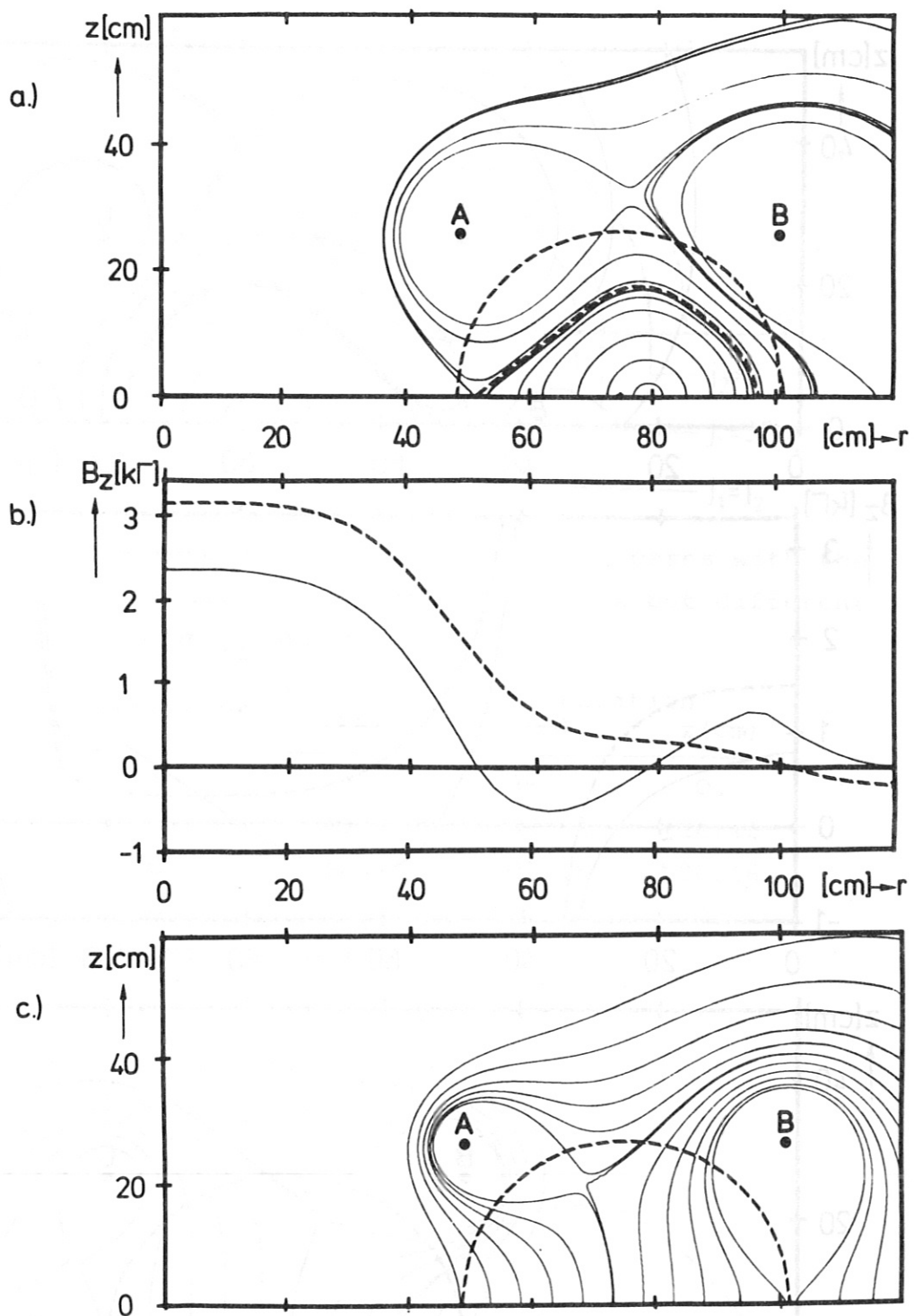


Fig.15 A compatible configuration obtained by iteration:

a) complete magnetic configuration,

b)  $B_z(r, z=0)$  without plasma current (dashed line)  
and including " " (solid " )

c) magnetic configuration produced by the multipole  
currents only.

The following currents and current densities are used:

Conductor	A	B	Plasma ( $J_0$ )
-----------	---	---	------------------

Current (kA)	154.7	42.7	-100
--------------	-------	------	------

current densities ( $\text{kA}/\text{cm}^2$ ):  $j_1 = -0.083$ ;  $j_2 = -0.011$



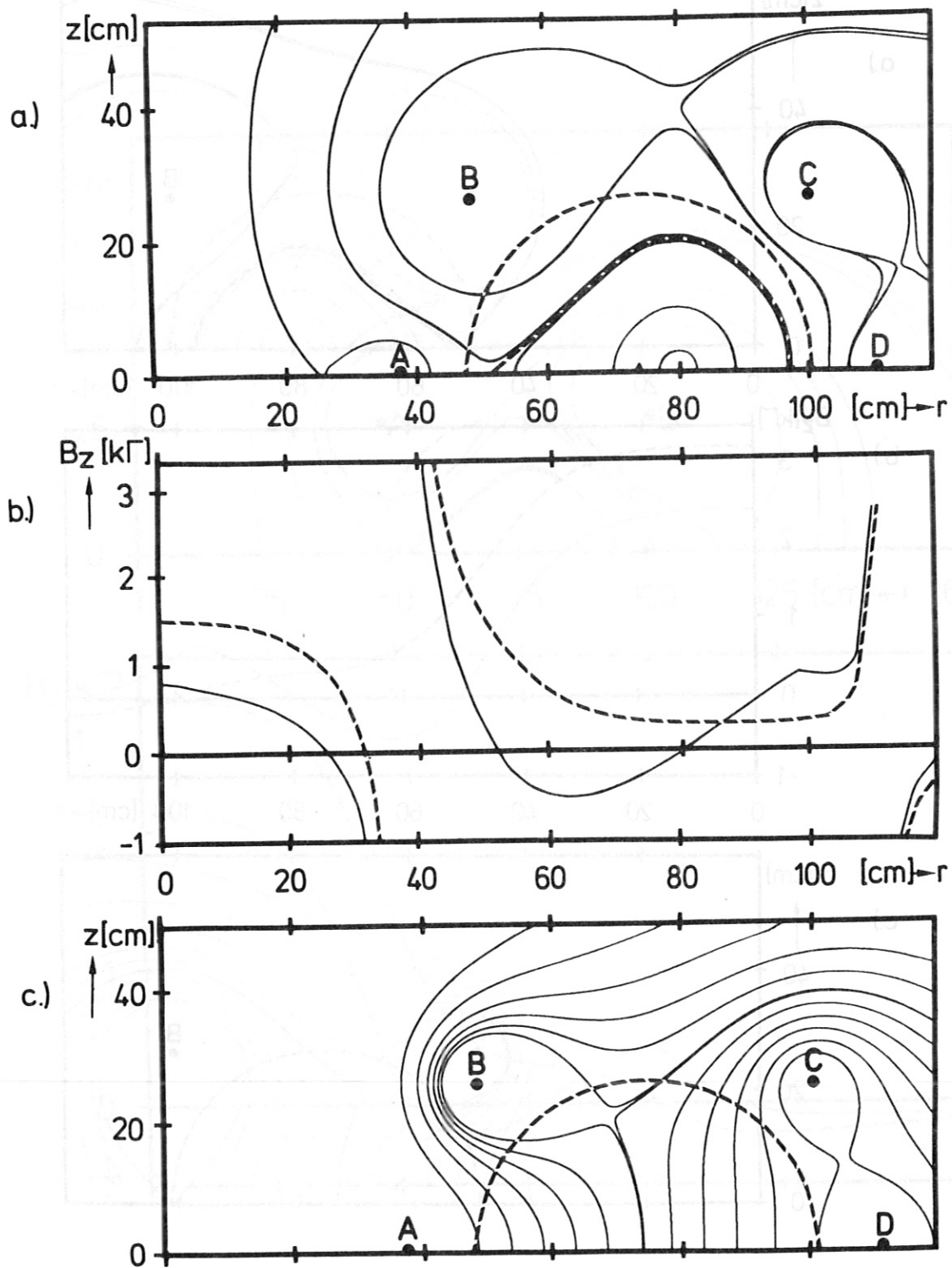


Fig.16 As fig.15, but with additional currents in the equatorial plane for better shaping of the plasma cross section:

Conductor	A	B	C	D	Plasma ( $J_0$ )
Current[kA]	-50.5	115.	21.4	14.2	-100
Current densities ( $\text{kA}/\text{cm}^2$ )	$j_1 = -0.073, j_2 = -0.011$				



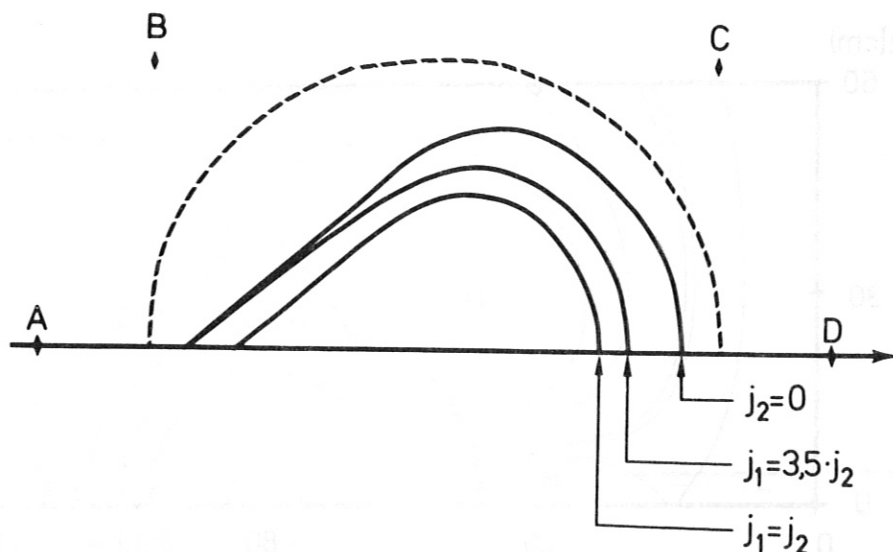


Fig.17 Three separatrices for compatible cases with the same plasma and multipole currents but different values of  $j_1$  and  $j_2$

Conductor	Current (kA)	Location	
		$r$ (cm)	$z$ (cm)
A	-50	38.	0.
B	120	48.84	$\pm 26.16$
C	22	101.16	$\pm 26.16$
D	17	112.	0.
Plasma	-100		

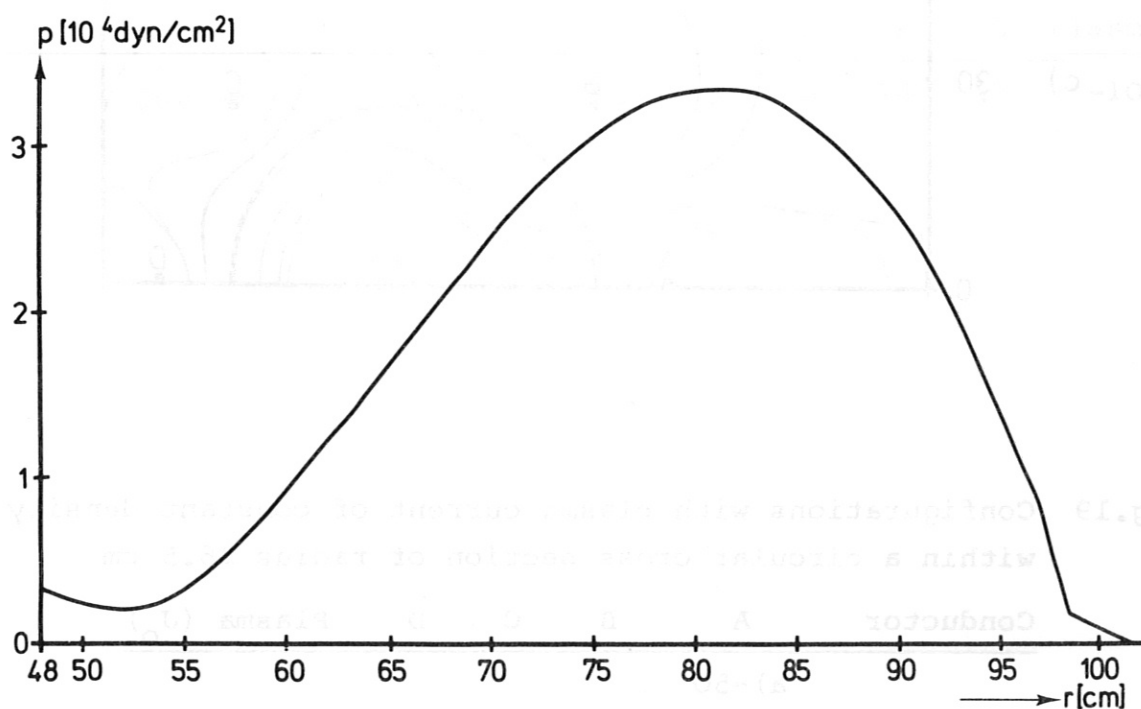


Fig.18 Plasma pressure in the equatorial plane, versus  $r$ , for the case in fig.16



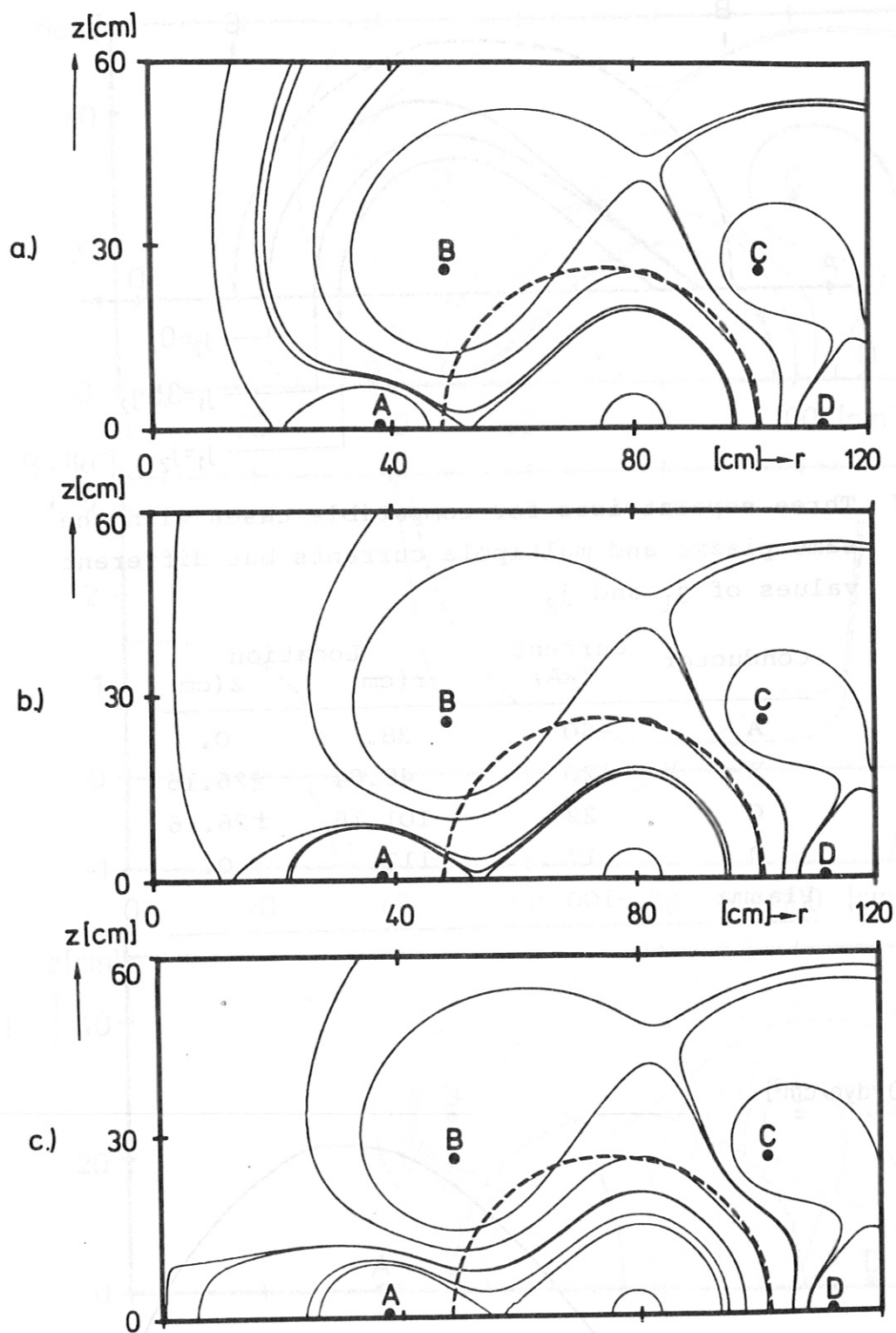


Fig.19 Configurations with plasma current of constant density within a circular cross section of radius 26.5 cm

Conductor	A	B	C	D	Plasma ( $J_0$ )
a) -50					
Current (kA) b) -65		100	17	20	-100
c) -80					



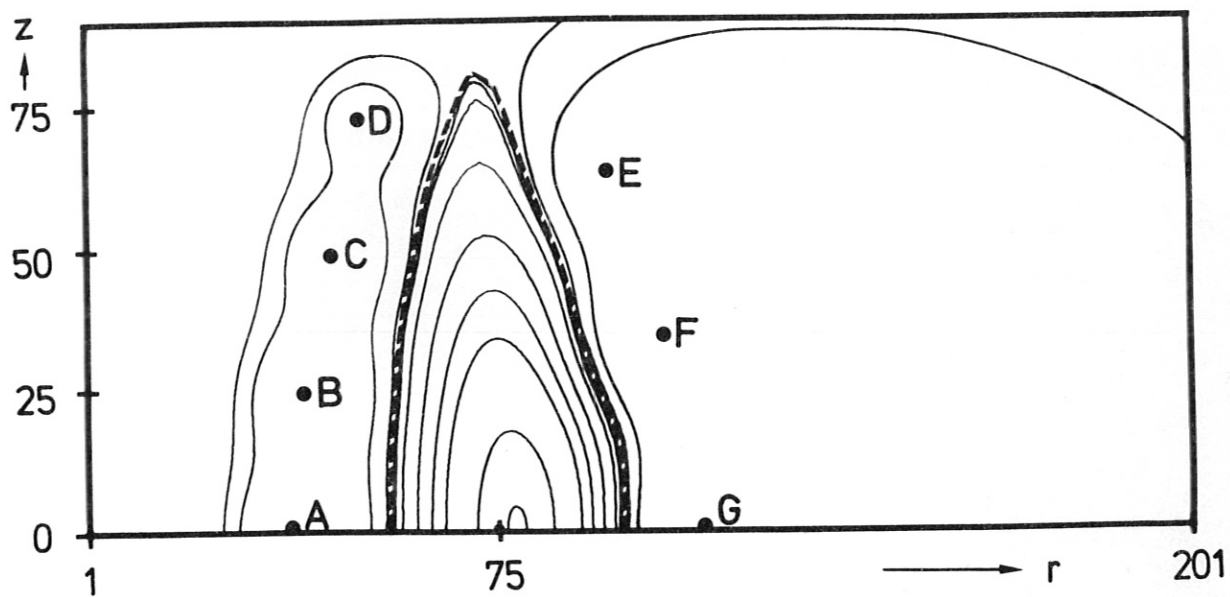


Fig.20 An example with elongated plasma cross section ( $J_0=100$  kA)

Conductor	A	B	C	D	E	F	G	Plasma( $J_0$ )
Current (kA)	35	30	20	15	8	14	12	-100